NSDHL MUTATIONS ASSOCIATED WITH CHILD SYNDROME IDENTIFIED IN ORAL VERRUCIFORM XANTHOMA

George I. Getz

A thesis submitted to the faculty of the University of North Carolina at Chapel Hill in partial fulfillment of the requirements for the degree of Master of Science in the School of Dentistry (Periodontology).

Chapel Hill
2018

Approved by:

Jonathan Reside

Antonio Amelio

Ricardo Padilla

Ingeborg De Kok

ABSTRACT

GEORGE I. GETZ: *NSDHL* Mutations Associated with CHILD Syndrome Identified in Oral Verruciform Xanthoma
(Under the direction of Jonathan Reside)

While the etiology of Verruciform xanthoma (VX) lesions remains unclear, recent evidence suggests the possible role of a mutation in the NAD(P)-dependent steroid dehydrogenase-like (*NSDHL*) gene in cutaneous lesions. The aim of this study is to evaluate the presence of mutations of the *NSDHL* gene in cases of oral VX.

A total of 112 oral VX lesions were diagnosed at the UNC Pathology Laboratory and Biopsy Service between 2005-2017. DNA was extracted from the archived formalin-fixed and paraffin tissue blocks in a subset of 20 patients. Polymerase chain reaction was then used to screen for the presence of four known germline mutations in the *NSDHL* gene associated with congenital hemidysplasia with ichthyosiform nevus and limb defects (CHILD) Syndrome and one somatic mutation that was identified in VX lesions in a previous study with no known CHILD syndrome association.

A total of eight of the tissue samples had known missense mutations associated with CHILD syndrome. Furthermore, two of these aforementioned eight tissue samples also had additional missense mutations previously identified in VX lesions. Thus, oral VX lesions may be associated with mutations in the *NSDHL* gene.

ACKNOWLEDGEMENTS

This dissertation would not have been possible without the guidance and assistance of many individuals who contributed to the preparation and completion of this study.

First and foremost, my utmost gratitude to my mentor Dr. Jonathan Reside and committee members Drs. Antonio Amelio, Ricardo Padilla, and Ingeborg De Kok whose encouragement and dedication has been my inspiration in the completion of this project.

Specifically, Dr. Amelio and his team: Mr. Kshitij Sharma, Ms. Adele Musicant, Dr. Miranda Carper, Ms. Shaily Aghera, Ms. Chloe Twomey, Ms. Saumya Goel, and Ms. Sophia Raterman for their guidance, assistance, and camaraderie during the bench research portion of this study.

Dr. Adam Lietzan for his assistance with the protein structure analysis.

Ms. Deanna DeCoursey at Eton Biosciences, Inc. for bearing with my numerous requests with the Sanger sequencing.

Co-residents Drs. Brenda Lopez, Bruno Herrera, and Megumi Williamson who helped me counter the tribulations of our residency life with a bit of humor.

My parents George and Carolinda for always supporting me in whatever my endeavor happened to be without question or judgment.

My wife Veronica for her encouragement, patience, and uncompromising smile.

TABLE OF CONTENTS

LIST OF TABLES

LIST OF FIGURES

LIST OF ABBREVIATIONS

CCR2	C-C chemokine receptor type 2
CHILD	Congenital Hemidysplasia with Ichthyosiform Erythroderma and Limb Defects
CI	Confidence Interval
CNS	Central nervous system
DNA	Deoxyribonucleic acid
H&E	Hematoxylin-eosin
HPV	Human Papillomavirus
mRNA	Messenger ribonucleic acid
MCP-1	Monocyte chemoattractant protein-1
NAD[P]H	Nicotinamide adenine dinucleotide phosphate
NSDHL	NAD[P]H steroid dehydrogenase-like protein
PCR	Polymerase chain reaction
PG	Poryphyromonas gingivalis
RNA	Ribonucleic acid
UNC	University of North Carolina
VX	Verruciform xanthoma

CHAPTER 1:

INTRODUCTION

VERRUCIFORM XANTHOMA

VX primarily affects the oral mucosa. First described by Shafer in 1971, it most commonly presents with a well-circumscribed verrucous or papillomatous appearance, however, in some instances VX may appear flat, polypoid or sessile (Shafer, 1971) (Figure 1). It usually occurs as a small (2mm–2cm), solitary, asymptomatic, slow growing, white, pink, grey, or yellowish lesion (Neville, 1986). Oral VX lesions are most commonly found on the gingiva (40.9-70.6%) (Philipsen et al., 2003), as well as the mandibular ridge, palate, floor of the mouth, lip, and mucobuccal fold (Shafer, 1971). Lesions have also been identified on the faucial pillars and the upper respiratory tract (Sathish et al., 2013; Travis et al., 1989). The differential diagnosis for oral VX includes squamous papilloma, verruca vulgaris, condyloma acuminatum, verrucous leukoplakia, squamous cell carcinoma, and gingival epulis (Qi et al., 2014). Histological evaluation following excisional biopsy is the primary means of diagnosis. Treatment via excision is usually curative for oral VX lesions as recurrence is rare (Shetty et al., 2013); only three recurrent cases have ever been described, and all were localized to the hard palate (Nowparast et al., 1981). In cutaneous VX, however, persistent recurrence is reported, although the condition eventually resolves (Connolly et al., 2003). No malignant transformation of VX has ever been reported, although two cases of oral VX were observed in association with carcinoma in situ and squamous cell

carcinoma, likely due to the degenerative epithelial changes in these oral lesions (Neville et al., 1986).

While the majority of oral VX lesions are isolated and solitary, multifocal lesions have been described in association with several diseases and conditions, including chronic graft-versus-host disease. However, multifocal lesions may also occur in otherwise healthy patients; four solitary gingival VX lesions were once identified in a patient with no systemic disease (Qi et al., 2014).

Extraoral VX lesions were first identified and described by Santa Cruz and Martin in 1979. Extraoral lesions are most commonly found involving the anogenital mucosa and epidermis, although lesions have also been identified on the penis and scrotum (Santa Cruz et al., 1979, Philipsen et al., 2003). In 2013, a 8mm diameter solitary VX lesion was found on the forearm of an 82-year-old male with an unremarkable medical history and no history of trauma to the area (Blankenship et al., 2013). Multiple extraoral VX lesions are usually associated with conditions such as epidermal nevi, lymphedema, and CHILD syndrome (Neville, 1986).

No data is available concerning the prevalence or incidence of oral VX. During the course of a 12-year period, 6 VX lesions were diagnosed from a total of 24,245 specimens in a university oral pathology laboratory setting, for a frequency of 0.025% (Buchner et al., 1981). In a 2002 literature review of 282 cases, oral VX occurred in females (mean age, 54.9 years) and males (mean age, 44.2 years) in a 1:1.1 female:male ratio. 109 out of the 282 cases were from Japanese patients, but a comparison with non-Japanese patients showed few discrepancies (Philipsen et al., 2003).

Histologically, in oral VX, the epithelium has a pebbly or verruciform surface, although it occasionally may appear flat (Nowparast et al., 1981). There is invagination of hyperkeratosis into crypts in the stratified squamous epithelium (Huang et al., 1986). Hematoxylin and eosin (H&E) staining of this parakeratin will produce a characteristic orange color, clearly separating the epithelium associated with the lesion from the surrounding epithelium. Often the parakeratinized surface will appear rough and will display infiltrations of neutrophils. Uniform elongation of rete pegs is characteristically present. However, the hallmark of VX is the presence of foamy (lipid-laden) cells, or xanthoma cells, within the connective tissue papillae between the rete ridges (Figure 2). These xanthoma cells do not usually extend deeper into the connective tissue than the tips of the rete pegs (Neville, 1980). Isolated foamy cells have also been noted within the epithelium in some cases (Cobb et al., 1976). Histologically, differentiation from other lesions that have foamy cells is not difficult as VX is the only lesion known to have these type cells confined to the connective tissue papillae (Shetty et al., 2013). Although there was some disagreement about the origin of the foam cells in the past, immunohistochemistry suggests that foam cells descend from macrophages, as they are positive for CD-68 and cathepsin B antibodies (Mostafa et al.,1993; Oliveira et al., 2001). Scattered lymphocytes and plasma cells may also be present in the connective tissue. Additional staining with Scharlach R stain has demonstrated the presence of lipid granules within the xanthoma cells and the overlying epithelium (Zegarelli et al., 1975). Periodic acid-Schiff positive, diastase-resistant granules have been found in the cytoplasm of the xanthoma cells (Shafer et al., 1971; Zegarelli et al., 1975; Santa Cruz et al., 1971). Occasionally, fungal hyphae or bacterial infiltrate may also

be identified (Mostafa et al., 1993), but it is thought that presence of these microbes most likely represents a secondary infection (Neville, 1980).

Electron microscopy of gingival oral VX lesions revealed the presence of lipid-laden macrophages (Zegarelli et al., 1975). A typical macrophage had an irregular nuclear profile with prominent nucleolus and the cytoplasm containing numerous large lipid vacuoles. Epithelial cell degeneration was evident with VX. Lipid containing vacuoles were identified in epithelial cells as well in the intercellular spaces between epithelial cells (Zegarelli et al., 1975). Light microscopy of cutaneous VX from the penis displayed numerous lipid vacuoles in melanocytes as well. Some of these were seen to be within the disrupted basal layer of the epithelium where they could reach the foam cells in the dermis (Balus et al., 1991).

There are a several theories on the etiology and pathogenesis of VX. Early on, noting that VX commonly occurs at areas of masticatory mucosa, it was proposed that epithelial degradation initiates formation of the characteristic foam cells (Zegarelli et al., 1975). The epithelium becomes entrapped with the crypts within the stratified squamous epithelium and is not lost from the body. The entrapped epithelium then degenerates, eventually forming lipids. The products of this breakdown elicit an inflammatory response, explaining the neutrophil infiltrate that is often seen within the epithelium and a mostly chronic cell infiltrate in the submucosa (Zegarelli et al., 1975). It is unclear, however, how the initial crypt that would necessitate the entrapment of epithelial cells form, although it is proposed it may be caused by a local irritant (Mehra et al., 2005). Later studies, however, observed foam cell deposition in areas of little epithelial degradation and without entrapment of epithelial cells (Travis et al., 1989). In a study of a multifocal VX in the upper aerodigestive tract of a child, three morphological manifestations of VX (verruciform, papillary, and flat) were

identified within the same individual. This suggested that the squamous epithelium progresses through flat and papillary stages, before becoming verrucous. Citing that macrophages are known to produce a variety of growth factors (Nathan, 1987), it was suggested that the foam cells might play a role in inducing epithelial hyperplasia. Therefore, it is believed that the accumulation of foam cells is the primary abnormality in the early lesion and that increasing epithelial hyperplasia and inflammation are secondary manifestations (Travis et al., 1989).

In order to discover the local factors that may regulate the recruitment and accumulation of the xanthoma cells in the connective tissue papilla, the cellular and molecular pathways of chronic inflammation have been studied using immunohistochemical techniques. It was suggested that keratinocyte hyperplasia may be initiated and maintained by T cell-mediated inflammation as a response to altered keratinocytes. Furthermore, they discovered MCP-1 localized in the basal layer of VX and CCR2 expressed in its foam cells. MCP-1 is a potent macrophage attractor and CCR2 up-regulates macrophage and T-cell trafficking. They suggested that this MCP-1/CCR2 axis may serve to induce macrophages in the sub-basal layer (Ide et al., 2008). This may explain why oral VX is most commonly identified on gingiva tissues, as gingivitis and chronic periodontitis are examples of T cell activation and keratinocyte expression of MCP-1. In fact, P. gingivalis can up-regulate the secretion of MCP-1 (Kuramitsu et al., 2002).

Lending further credence that VX may be the result of a chronic inflammatory process, Rawal et al., 2007, in the first study of its kind, characterized the phenotypes of the foam cells in VX at different oral locations. They found that the resident and chronic inflammatory reparative macrophage subtypes far outnumbered the acute inflammatory foam

cells, consistent with a chronic reactive process. This was found consistently, regardless of the location of the VX lesions.

The source of the lipid contained in foam cells has been the subject of investigation, in the hope that this may lead to the identifying the pathophysiology of VX. It has been suggested by some (Huguet et al., 1995; Kishimoto et al., 1998; Wu et al., 2003) that it may derive from serum lipoprotein. However, squamous epithelium are active sites of lipid biosynthesis (Ide et al., 1998), these lipids increase in conditions of chronic inflammatory dermatoses (Uchiyama et al., 2000), and the ultrastructure of VX reveals membrane-bound lipid-laden vacuoles and foamy macrophages within the epithelium (Zegarelli et al., 1975). Therefore, it appears that the theory that the degradation of the epithelium, and the resultant uptake of the keratocyte's lipids by macrophages in the dermis, may, in fact, lead to the formation of the pathognomonic foam cells of VX (Balus et al., 1991).

As the clinical manifestation is often verruciform or papillary, and common locations for VX are the oral cavity or genitalia, a viral etiology, and specifically Human Papilloma Virus (HPV), has been suggested (Mehra et al., 2005). However, multiple studies have failed to prove such a connection. While HPV DNA has been found in condyloma-appearing VX (Hu et al., 2005) and one case report found an association between HPV type 6a particles found in the nucleus of keratinocytes of a cutaneous VX (scrotum) lesion after PCR and sequence analysis (Khaskhely et al., 2000), no signs of HPV *infection* have ever been detected.

There are several other diseases and syndromes that have shown an association with VX. There is one case study where an association was found with both a rare type of congenital lymphedema, chronic hereditary lymphedema ("Milroy Disease"), and leaky

capillary syndrome, a condition where vascular permeability leads to hemodynamic disorder. The locations of the multifocal papillary lesions in both cases were in the lower extremities. It was reasoned that accumulation of lipids in subcutaneous tissues gave rise to the characteristic foamy cells in their patient's VX, the result of atypical peripheral lymphatics and permeable capillaries, allowing exudation into subcutaneous tissue. Indeed, Hunter et al. proposed this mechanism for VX in 1970 (Wu et al., 2003).

More recently, VX has been associated with CHILD syndrome, a rare x-linked autosomal dominant disorder caused by a mutation of the NAD[P]H steroid dehydrogenase-like (*NSHDL*) gene involved in cholesterol biosynthesis (Mehra et al., 2005). The lesions in CHILD syndrome and VX have a similar morphological and histological appearance, including the appearance of foam cells confined to the connective tissue papillae. The authors surmised that this inactivation of the *NSDHL* gene also plays a role in sporadic VX.

NAD[P]H STEROID DEHYDROGENASE-LIKE (NSHDL) GENE

Cholesterol is a major precursor of steroid hormones, influencing embryonic and postnatal development. The *NSHDL* gene encodes for a 3b-hydroxysteroid dehydrogenase located within the membranes of endoplasmic reticulum and on the surface of intracellular lipid storage droplets that is involved in one the later steps of the biosynthesis pathway of cholesterol, where C-4 methyl groups are removed (Caldas et al., 2003; Preiksaitene et al., 2015). Its chromosomal location is on the long arm of the X chromosome at position 28 (Xq28). *NSHDL* has 8 exons (Figure 3) encoding an mRNA of 1581 base pairs, with the first methionine codon located at exon 2. The encoded NSDHL protein is composed of 373 amino acid residues. Mutation of the *NSHDL* leads to abnormalities in the pathway of

cholesterol synthesis. A disruption of the expression of this gene can manifest itself in the lack of formation and maintenance of an intact cutaneous barrier, explaining, among other sequelae, the ichthyosiform erythroderma that are characteristic for CHILD syndrome (Mi et al., 2015). Loss of function mutations in *NSHDL* also cause an even more rare congenital disease, CK syndrome (Morimoto et al., 2011; Kanungo et al., 2013).

CONGENITAL HEMIDYSPLASIA WITH ICHTHYOSIFORM NEVUS AND LIMB DEFECTS (CHILD) SYNDROME

CHILD syndrome is a rare x-linked dominant syndrome, with only 60 cases reported worldwide (Souich et al., 2015). It is a multisystem birth defect that is usually male-lethal, with only one documented male case likely due to postzygotic mutation (Happle et al., 1996). First described in 1903 by Otto Sachs, symptoms usually present at birth or within the first few weeks of development (Bittar and Happle, 2004). It is usually characterized by an inflammatory epidermal nevus with an often wax-like scaling showing a unique lateralization pattern (usually on the right side) (Hummel et al., 2003) and a midline demarcation, although a single case has been found with symmetrical skin lesions (König et al., 2002). In addition, structural defects may be found ipsilateral to major cutaneous involvement, including hearing loss, the shortening or absence of limbs and hypoplasia of the brain, lung, heart, and the kidney (Happle et al., 1980; König et al., 2002). It has been hypothesized that the unilateral manifestations in CHILD Syndrome could result from interference by mutant cells with a small population of organizer cells determining the laterality decision at the midline (Hummel et al., 2003).

Because of the typical clinical and histopathological aspects of the CHILD syndrome nevus, a diagnosis can be made in classic cases and also in those cases with only minimal

involvement. CHILD syndrome has been diagnosed in patients with only the ipsilateral lesions, with no ipsilateral skeletal defects (Ko et al., 2008). Female carriers may occasionally be found clinically healthy or only having minimal involvement due to X-inactivation (lyonization) or skewed X-inactivation (McLarren et al., 2010, Yu et al., 2018). As a result, numerous sporadic occurrences of CHILD syndrome may be found to be familial cases after genetic testing (Bittar et al., 2006).

Histology of the CHILD syndrome lesions show similar structures as found in VX. A typical epidermal lesion will display acanthosis and marked parakeratosis with lymphocyte infiltration involving the upper part of the dermis and a considerable number of neutrophils present in the epidermis. Finally, the dermal papillae contain considerable numbers of foamy cells (Happle et al., 1996). These similarities were even seen in a mild case of CHILD syndrome. A biopsy from a persistent VX appearing lesion from the left side of the vulva (a common location for extraoral VX lesions) of an otherwise asymptomatic 27-year old female revealed a broad parakeratotic corneal layer, neutrophil aggregation, and foam cells in the dermal papillae. Molecular analysis confirmed a mutation of the *NSDHL* consistent with those seen in CHILD syndrome (Gantner et al., 2014).

Mutations in the *NSDHL* at the Xq28 chromosome locus were identified as the likely cause for CHILD syndrome (König et al., 2000). Soon after, 4 different mutations of the NSDHL gene were reported in subjects with CHILD syndrome (Bornholdt et al., 2005), and, to date, 20 unique mutations at different exons in the NSDHL gene have been found to cause CHILD syndrome (Mi et al., 2015). While the majority of these mutations have been missense or nonsense mutations, cases with frameshift mutations, splice-site mutations, and large deletions of multiple exons have also been documented (Bornholdt et al, 2005; Kim et

al., 2005; Yu et al., 2018, Yang et al., 2015). The mutations have also been reported at all 8 exons in various studies (Mi et al., 2015). Although there is great variability in the sequelae of CHILD syndrome, phenotypic variability does not appear to be associated with a specific type or location of the mutations. The end result of any type of mutation appears to be loss of function for the enzyme. It is believed that a non-functional NSDHL may cause the characteristics of CHILD syndrome through the resulting lack of cholesterol, other sterols downstream of the block in biosynthesis, or by accumulations of intermediate products upstream of the resultant of NSDHL expression (Bornholdt et al., 2005). Abnormalities in cholesterol synthesis would be significant as cholesterol plays a role in the establishment and upkeep of a complete cutaneous barrier. Accumulation of the toxic pathway metabolites could also contribute to the characteristic ichthyosis. In one study, a compounded lovastatin and cholesterol topical medication wad designed to treat CHILD syndrome lesions by bypassing hepatic first-pass metabolism and allowing access to cutaneous and extracutaneous tissues). This was compared to a purely cholesterol-based control treatment (Paller et al., 2011). The treatment with cholesterol alone did not resolve the lesions. However, the addition of the statin appeared to address the toxic metabolites while the supplemental cholesterol countered the cholesterol deficiency. Following 3 months of treatment, the previously affected epidermis was of normal thickness, with a regular orthokeratinization and normal stratum granulosum (Mi et al., 2015.

CK SYNDROME

CK Syndrome, named for the initials of an affected patient, is an intellectual disability disorder characterized by disparate short height, brain malformations, and

dysmorphia (Souich et al., 2009). Only 24 cases, from 3 unrelated families, have been identified, and its prevalence is unknown (Souich et al., 2015). Like CHILD syndrome, it is an x-linked disorder where the primary etiology is dysfunction of the NSDHL gene at the Xq28 chromosome. Unlike the x-linked dominant disease CHILD syndrome, it is inherited in a recessive manner, affecting males, and its primary sequelae are mild to severe intellectual disability, behavior problems (aggression, attention deficit hyperactivity disorder, and irritability), and dysmorphia including amygdaliform eyes, a high nasal bridge, high arched palate, long and slender fingers and toes, scoliosis, micrognathia, and a crowded dentition (Souich et al., 2009; Morimoto et al., 2012; Kanungo et al., 2013). The different clinical phenotypes may be explained because of the different alleles of the NSDHL gene. CHILD syndrome patients have null alleles that result in the complete loss of function of NSDHL. On the other hand, in CK Syndrome, patients possess hypomorphic temperature-sensitive alleles that result in the partial loss of the functional NSHDL protein (McLarren et al., 2010). The exact process by which this occurs is unclear. The use of quantitative reverse transcriptase PCR, immunoblotting, and immunohistochemistry to determine NSDHL protein expression in peripheral tissues identified NSDHL expression in all non-CNS tissues with malformations in CK syndrome (and CHILD syndrome) (Morimoto et al., 2012). Indeed, all of these tissues have been shown to synthesize cholesterol. Furthermore, this established that NSHDL gene expression was restricted to specific cells within the tissues. Autonomous and non-autonomous cellular mechanisms could occur because of impairment of the normal biological processes by cholesterol deficiency, toxicity of cholesterol biosynthesis intermediates or their metabolites. This may contribute to the particular features of CK Syndrome and CHILD syndrome.

IMPLICATIONS OF IDENTIFYING THE ROLE OF THE NSDHL GENE IN ORAL VERRUCIFORM XANTHOMA

A previous study was conducted to identify direct associations between CHILD syndrome and Verruciform xanthoma (Mehra et al., 2005). The lesions were perioral or extraoral, including the labium, groin, scrotum, thigh, calf, abdomen, and upper lip. While missense mutations that had been reported for CHILD syndrome were not identified, a different missense mutation in a common exon (exon 6) of the NSDHL gene was identified in 2 out the 7 patients included in the study. To date, no association between the mutations that cause CHILD Syndrome and oral VX lesions has been researched.

VX cutaneous lesions are associated with CHILD syndrome. As the syndrome is caused by mutations of the NSDHL gene, there is a possibility that oral VX lesions may also be associated with a mutation in the NSDHL. Any mutations noted may help to establish an etiologic theory for VX and support further efforts to evaluate risk of NSDHL mutations in sterol metabolism disorders like CHILD syndrome or CK syndrome in families with oral VX.

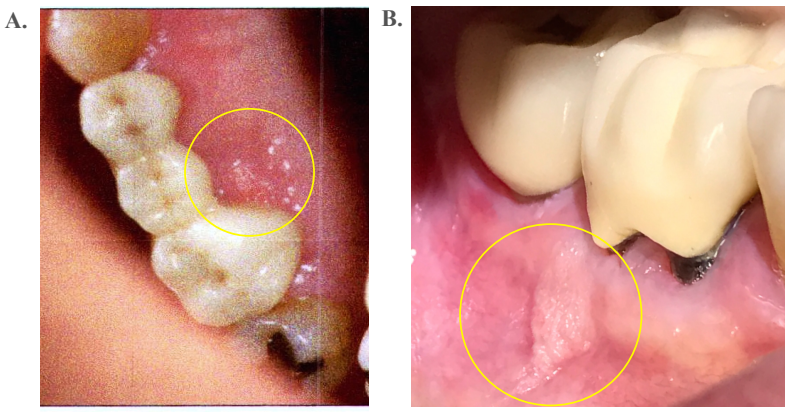

Figure 1. Clinical Photographs Submitted with Tissue Biopsies to UNC Oral Pathology Laboratory and Biopsy Service. (A) Test Sample 4. (B) Test Sample 9.

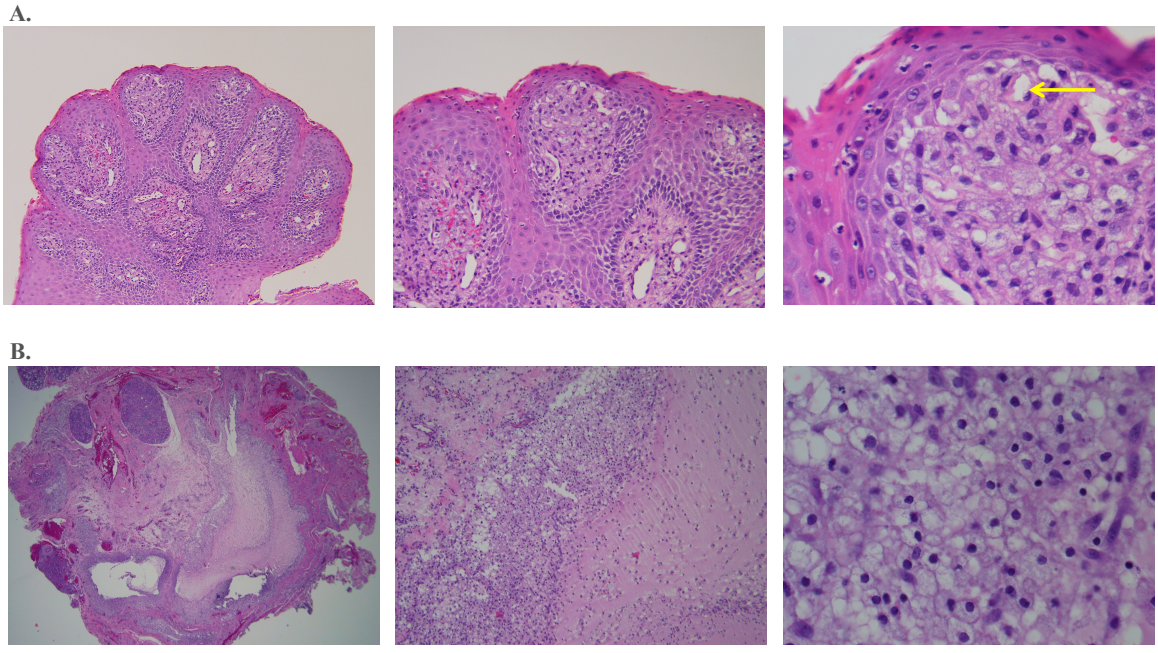

Figure 2. Histologic Images from Oral Verruciform Xanthoma and Oral Mucocele Lesions (H&E Staining). (A) Test Sample 16 at increasing magnification (xanthoma cell indicated by arrow). (B) Control Sample 1 (oral mucocele).

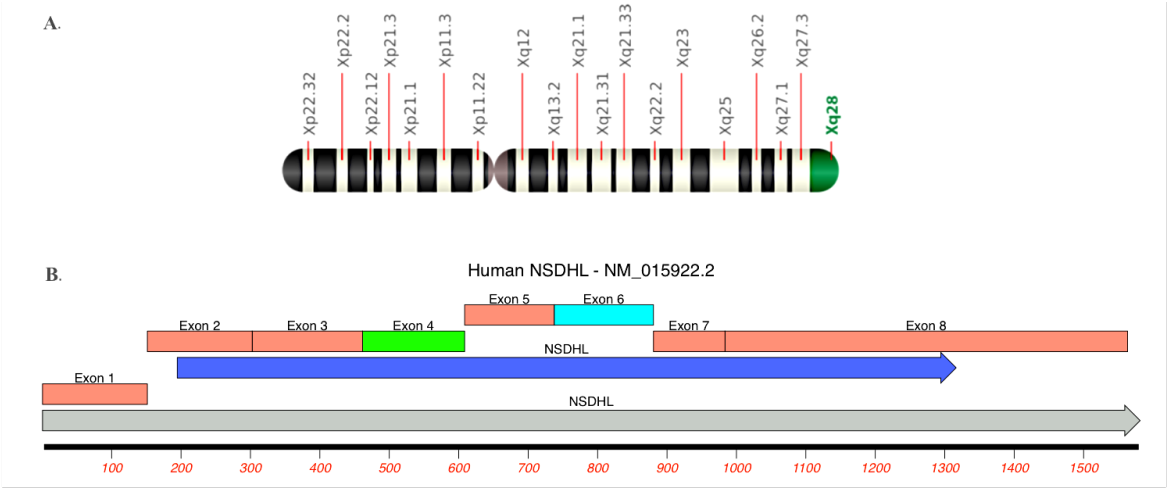

Figure 3. NSDHL Gene. (A) Gene location on the long arm of the X chromosome at position 28. (B) Exons of the NSDHL gene.

REFERENCES

Balus, Breathnach AS, O'Grady AJ. Ultrastructural observations on "foam cells" and the source of their lipid in verruciform xanthoma. J Am Acad Dermatol. 1991;24(5):760-764.

Bittar M, Happle R. CHILD syndrome avant la lettre. J Am Acad Deratol. 2004;50(2 Suppl):S34-37.

Bittar M, Happle R, Grzeschik K-HH, Leveleki L, Hertl M, Bornholdt D, et al. CHILD syndrome in 3 generations: the importance of mild or minimal skin lesions. Arch Dermatol. 2006;142(3):348-351.

Blankenship W, Zech L, Mirzabeigi M, Venna S. Verruciform xanthoma of the upper-extremity in the absence of chronic skin disease or syndrome: a case report and review of the literature. J Cutan Pathol. 2013;40(8):745-752.

Bornholdt D, König A, Happle R, Leveleki L, Bittar M, Danarti R, et al. Mutational spectrum of NSDHL in CHILD syndrome. J Med Genet. 2005;42(2):e17.

Buchner A, Hansen LS, Merrell PW. Verruciform xanthoma of the oral mucosa. Report of five cases and review of the literature. Arch Dermatol. 1981;117:563-565.

Caldas H, Herman GE. NSDHL, an enzyme involved in cholesterol biosynthesis, traffics through the Golgi and accumulates on ER membranes and on the surface of lipid droplets. Hum Mol Genet 2003;12:2981-2991.

Cobb CM, Holt R, Denys FR. Ultrastructural features of the verruciform xanthoma. J Oral Pathol. 1976; 5:42-51.

Connolly SB, Lewis EJ, Lindholm JS, Zelickson BD, Zachary CB, Tope WD. Management of cutaneous verruciform xanthoma. J Am Acad Dermatol. 2000;42(2 Pt 2):343–347.

Gantner S, Rütten A, Requena L, Gassenmaier G, Landthaler M, Hafner C. CHILD syndrome with mild skin lesions: histopathologic clues for the diagnosis. J Cutan Pathol. 2014;41(10):787–790.

Happle R, Koch H, Lenz W. The CHILD syndrome: congenital hemidysplasia with ichthyosiform erythroderma and limb defects. Eu K Pediatr. 1980; 134:27-33.

Happle R, Effendy I, Megahed M, Orlow S, Küster W. CHILD syndrome in a boy. Am J Med Genet. 1996;62(2):192–194.

Hegde U, Doddawad V, Sreeshyla, Patil R. Verruciform xanthoma: A view on the concepts of its etiopathogenesis. J Oral Maxillofac Pathology. 2013;17(3):392-396.

Huang JS, Tseng CC, Jin YT, Huang CC, Wong TY, Chen HA, et al. Verruciform xanthoma. Case report and literature review. J Periodontol. 1996;67(2):162-165.

Huguet P, Toran N, Tarragona J. Cutaneous verruciform xanthoma arising on a congenital lymphoedematous leg. Histopathology. 1995;26(3):277-279.

Hummel M, Cunningham D, Mullett C, Kelley R, Herman G. Left-sided CHILD syndrome caused by a nonsense mutation in the NSDHL gene. Am J Med Genet A. 2003;122A(3):246-251.

Hunter JAA, Morely WN, Peterkin GAG. Xanthomatosis secondary to lymphedema. Trans St John Hosp Dermatol Soc. 1970;56:143-148.

Ide F, Obara K, Yamada H, Mishima K, Saito I, Kusama K. Cellular basis of verruciform xanthoma: immunohistochemical and ultrastructural characterization. Oral Dis. 2008;14(2):150-157.

Khaskhely NM, Uezato H, Kamiyama T, Maruno M, Kariya KI, Oshiro M, Nonake S. Association of human papillomavirus Type 6 with a verruciform xanthoma. Am J Dermatopathol. 2000;22(5):447-452.

Kishimoto S, Takenaka H, Shibagaki R, Nagata M, Katoh N, Yasuno H. Verruciform xanthoma arising in an arteriovenous haemangioma. Br J Dermatol. 1998 Sep 2;139(3):546-548.

Kanungo S, Soraes N, Steiner RD. Sterol metabolism disorders and neurodevelopment-an update. Dev Disabil Res Rev. 2013;17(3):197-210.

Ko JY, Shin, Lee CW. A verruciform xanthoma-like phenomenon in a linear epidermal naevus in the absence of a syndromic association. Br J Dermatol. 2008;159(2):493-496.

König A, Happle R, Bornholdt D, Engel H, Grzeschik KH. Mutations in the NSDHL gene, encoding a 3beta-hydroxysteroid dehydrogenase, cause CHILD syndrome. Am J Med Genet. 2000;90(4):339-346.

Kuramitsu HK, Miyakawa H, Qi M, Kang IC. Cellular responses to oral pathogens. Ann Periodontol. 2002;7(1):90-94.

McLarren K, Severson T, Souich C du, Stockton D, Kratz L, Cunningham D, et al. Hypomorphic Temperature-Sensitive Alleles of NSDHL Cause CK Syndrome. Am J Hum Genetics. 2010;87(6):905-914.

Mehra S, Li L, Fan C-YY, Smoller B, Morgan M, Somach S. A novel somatic mutation of the 3beta-hydroxysteroid dehydrogenase gene in sporadic cutaneous verruciform xanthoma. Arch Dermatol. 2005;141(10):1263-1267.

Mi X, Luo M, Guo L, Zhang T, Qiu X. CHILD Syndrome: Case Report of a Chinese Patient and Literature Review of the NAD[P]H Steroid Dehydrogenase-Like Protein Gene Mutation. Int Congr Ser. 2015;32(6):e277-e282.

Morimoto M, Souich C, Trinh J, McLarren K, Boerkoel C, Hendson G. Expression profile of NSDHL in human peripheral tissues. J Mol Histol. 2012;43(1):95-106.

Mostafa KA, Takata T, Ogawa I, Ijuhin, Nikai H. Verruciform xanthoma of the oral mucosa: a clinicopathological study with immunohistochemical findings relating to pathogenesis. Virchows Arch A Pathol Anat Histopathol. 1993;423(4):243-248.

Nathan C. Secretory products of macrophages. J Clin Invest. 1987;79(2):319-326.

Neville B, Weathers D. Verruciform xanthoma. Oral Surg Oral Medicine Oral Pathology. 1980;49(5):429-434.

Neville B. The verruciform xanthoma. A review and report of eight new cases. Am J Dermatopathol. 1986;8(3):247-253.

Nowparast B, Howell F, Rick G. Verruciform xanthoma A clinicopathologic review and report of fifty-four cases. Oral Surg Oral Medicine Oral Pathology. 1981;51(6):619-625.

Oliveira PT, Jaeger RG, Cabral LAG, Carvalho YR, Costa ALL, Jaeger MMM. Verruciform xanthoma of the oral mucosa. Report of four cases and a review of the literature. Oral Oncol. 2001;37(3):326-331.

Paller A, Steensel M, Rodriguez-Martín M, Sorrell J, Heath C, Crumrine D, et al. Pathogenesis-Based Therapy Reverses Cutaneous Abnormalities in an Inherited Disorder of Distal Cholesterol Metabolism. J Invest Dermatol. 2011;131(11):2242-2248.

Philipsen HP, Reichart PA, Takata, Ogawa. Verruciform xanthoma—biological profile of 282 oral lesions based on a literature survey with nine new cases from Japan. Oral Oncol. 2003;39(4):325-336.

Preiksaitiene E, Caro A, Benušienė E, Oltra S, Orellana C, Morkūnienė A, et al. A novel missense mutation in the NSDHL gene identified in a Lithuanian family by targeted next-generation sequencing causes CK syndrome. Am J Med Genet A. 2015;167(6):1342-1348.

Qi Y, Sun Q, Yang P, Song A. A case of multiple verruciform xanthoma in gingiva. Br J Oral Maxillofac Surg. 2014;52(1):e1-e3.

Rawal S, Kalmar J, Tatakis D. Verruciform Xanthoma: Immunohistochemical Characterization of Xanthoma Cell Phenotypes. J Periodontol. 2007;78(3):504-509.

Santa Cruz DJ, Martin SA. Verruciform xanthoma of the vulva. Report of two cases. Am J

Clin Pathol. 1979;7: 224-8.

Sathish, Suhas, Ch, Shekar, Praveen, Sachin G, et al. Verroucas Xanthoma of Faucial Pillar - A Case Report. Otolaryngology Open Access. 2013;3(4).

Shafer W. Verruciform xanthoma. Oral Surg Oral Medicine Oral Pathology. 1971;31(6):784-789.

Shetty A, Nakhaei K, Lakkashetty Y, Mohseni M, Mohebatzadeh I. Oral Verruciform Xanthoma: A Case Report and Literature Review. Case Reports Dent. 2013:528967.

Souich C du, Chou A, Yin J, Oh T, Nelson T, Hurlburt J, et al. Characterization of a new X-linked mental retardation syndrome with microcephaly, cortical malformation, and thin habitus. Am J Med Genet A. 2009;149A(11):2469-2478.

Souich C du, Raymond, FL, Grzeschik KH, Boerkoel CF. NSDHL-related disorders. GeneReviews [Internet]. Seattle (WA): University of Washington, Seattle; 2015.

Tarpey P, Smith R, Pleasance E, Whibley A, Edkins S, Hardy C, et al. A systematic, large-scale resequencing screen of X-chromosome coding exons in mental retardation. Nat Genet. 2009;41(5):ng.367.

Travis WD, Davis GE, Tsokos M, Lebovics R, Merrick HF, Miller SP, et al. Multifocal verruciform xanthoma of the upper aerodigestive tract in a child with a systemic lipid storage disease. Am J Surg Pathol. 1989;13(4):309-316.

Uchiyama N, Yamamoto A, Kameda K, Yamaguchi H, Ito M. The activity of fatty acid synthase of epidermal keratinocytes is regulated in the lower stratum spinousum and the stratum basale by local inflammation rather than by circulating hormones. J Dermatol Sci. 2000;24(2):134-141.

Wu JJ, Wagner AM. Verruciform xanthoma in association with milroy disease and leaky capillary syndrome. Pediatr Dermatol. 2003;20(1):44-47.

Yang Z, Hartmann B, Xu Z, Ma L, Happle R, Schlipf N, et al. Large deletions in the NSDHL gene in two patients with CHILD syndrome. Acta Derm-venereol. 2015;95(8):1007-1008.

Yu X, Zhang J, Gu Y, Deng D, Wu Z, Bao L, et al. CHILD Syndrome Mimicking Verrucous Nevus in a Chinese Patient Responded Well to The Topical Therapy of Compound of Simvastatin and Cholesterol. J Eur Acad Dermatol. 2018; Jan 17. doi:10.1111/jdv.14788.

Zegarelli DJ, Zegarelli-Schmidt EC, Zegarelli EV. Verruciform xanthoma. Further light and electron microscopic studies, with the addition of a third case. Oral Surg Oral Med Oral Pathol. 1975;40(2):246-256.

CHAPTER 2:

NSDHL MUTATIONS ASSOCIATED WITH CHILD SYNDROME IDENTIFIED IN ORAL VERRUCIFORM XANTHOMA

INTRODUCTION

Verruciform xanthoma (VX) is an uncommon benign lesion, commonly papillomatous or verruciform, which has an unknown etiology and is seen primarily in the oral mucosa (Hegde et al., 2013). A mutational inactivation of the NAD[P]H steroid dehydrogenase-like protein (NSDHL) gene has been reported in cutaneous VX (Mehra et al., 2015). Lesions resembling VX clinically and morphologically are found in subjects with the X-linked dominant lipid storage disease congenital hemidysplasia with ichthyosiform erythroderma and limb defects (CHILD) (Mi et al., 2015). The mutational inactivation of the NSDHL gene is a marker for CHILD as well as another lipid storage disease, CK syndrome (McLarren et al., 2010). Between July 2005 and 2017, 112 cases of oral VX were diagnosed at the University of North Carolina Oral Pathology Laboratory and Biopsy Service. We proposed to look for a NSDHL gene mutation in diagnosed oral VX cases to begin to establish a possible etiological theory for this lesion, and eventually support further efforts to evaluate for risk for CHILD or CK syndromes in families with patients with oral VX.

MATERIALS AND METHODS

Archived Samples Collection

Twenty-five formalin-fixed and paraffin-embedded (FFPE) tissue blocks were retrieved from the UNC Oral Pathology Laboratory and Biopsy Service using consecutive sampling. The accession dates ranged from to July 2015 to December 2017. Twenty of the test samples had been previously diagnosed as oral Verruciform xanthoma and five samples that had been diagnosed as oral mucoceles served as negative controls. Each sample came from a unique human subject.

DNA Extraction from Samples

Five tissue sections (5 μm thick) were produced with a microtome from each selected FFPE block. Each sample was deparaffinized with one 1 mL wash of 100% xylene followed by one 1 mL wash in 100% ethanol. The deparaffinized tissues were then subjected to DNA extraction using the EX-WAX Paraffin-Embedded DNA Extraction Kit (Millipore Sigma, Darmstadt, Germany), according to manufacturer's instruction. DNA concentrations and 260/280 and 260/230 ratios were assessed using a DeNovix DS-11 spectrophotometer (DeNovix, Wilmington, DE). Each DNA sample and its dilution to a 100ng/μL concentration (when possible) were stored at -20ºC.

Plasmid Construction

A plasmid was designed and subsequently constructed by Invitrogen GeneArt Synthesis (Thermo Fisher Scientific, Regensburg, Germany) to include mutations of interest previously reported in the literature from Exon 4 and Exon 6 of the *NSDHL*, including C>T =

A105V within Exon 4 and G>C = A182P, G>A = R199H, and G>A = G205S within Exon 6. G>A = R199H was associated with a somatic mutation found in Verruciform xanthoma tissues and the others have been reported as associated with CHILD Syndrome (Mehra et al., 2005) (Figures 4, 5). The plasmid was cloned into the pcDNA3.1_V5-HistA_A122 vector and the gene size was 1131 bp. 5µg of the lyophilized DNA was dissolved in 50µL of distilled water. Transformation was accomplished with DH5-alpha competent cells (Thermo Fisher Scientific, Durham, NC) according to manufacturer's instructions. After overnight incubation at 37ºC, the plasmid was recovered using the NucleoSpin Plasmid miniprep kit (Macherey-Nagel GmbH & Co., Duren, Germany). The plasmid and its dilution to a 75ng/µL concentration were stored at -20ºC. The plasmid, which would include the mutations of interest was constructed for comparison with test samples after spiking into a control sample. This combination would serve as a positive control.

Polymerase Chain Reaction Amplification of Exons 4 and 6 of the NSDHL gene

Primer sets were designed to amplify mutations reported in the literature within exons 4 and 6 of the *NSDHL* gene (Eton Biosciences, Research Triangle Park, NC) (Mehra et al., 2005). These include C>T = A105V within Exon 4 and G>C = A182P, G>A = R199H, G>A = G205S, and C>T = Q210X within Exon 6. The primer sequences are 5'-CCA GCT CTG AAA GGT GTA AAC ACA-3' (sense) and 5'-CAA GTT TCA ATG ACA TTC TTG GTG CC-3' (antisense) for exon 4; 5'-A GTT CTG GGC GCC AAC GAT-3' (sense) and 5'-CAA TCA CGA ACT TCA TCT TGC CGT-3' (antisense) for exon 6. We later designed an additional primer – an intron 5 primer (5' - GCA CTC TCT TGG CTT GGG – 3' (sense)) - to pair with the previously described exon 6 (antisense) primer to capture an additional

mutation described in the literature for CHILD Syndrome, G>C = A182P (Mehra et al., 2005). All primer pairs were verified via visualization by electrophoresis on 1.5% agarose gels using HEK293T as a DNA template. The plasmid itself was verified via amplification with the exon 4 (sense) and exon 6 (antisense) primer pairs (amplicon size of 409bp). The expected size of polymerase chain reaction (PCR) amplicons with the test and controls samples is 119 base pairs for exon 4 sense/antisense primers, 140 base pairs for exon 6 sense/antisense primers, and 206 base pairs for intron 5 (sense)/exon 6 antisense primers.

Each amplification was carried out in a Bio-Rad T100 Thermal Cycler (Bio-Rad Laboratories, Hercules, CA) in a 50-µL PCR mixture containing: 600ng genomic DNA, 5µL(50µM) of each sense and antisense primer, 25µl Maxima Hot Start PCR Master Mix (2X) (composition: 400µM dATP, 400µM dGTP, 400µM dCTP, 400µM dTTP, 4mM magnesium chloride, Maxima Hot Start Taq DNA polymerase in 2X PCR buffer (Thermo Fisher Scientific, Durham, NC)), and DNase/RNase-free distilled water.

The 20 test samples (designated T1-T20) and the 5 negative controls (designated C1-C5) were amplified with exon 4 primer pairs, the exon 6 primer pairs, and the intron 5/exon 6 (antisense) primer pairs. The plasmid was amplified with exon 4 sense and exon 6 antisense primers. As mentioned previously, one of the control samples (C5) spiked with the plasmid (C5-PL) and amplified with the same primer pairs served a positive control. Thermocycling conditions used were initial denaturation and hot start at 95°C for 15 minutes, 40 cycles consisting of 30 seconds at 95°C, 30 seconds at 60°C, and then 1 minute at 72°C. Following thermocycling, reactions were subjected to a 5-minute 72°C incubation. Polymerase chain reaction amplicons were visualized by electrophoresis on 2.0% agarose gels and with Gel Red (Biotium, Fremont, CA) staining. After UV transillumination, selected bands

corresponding to the aforementioned base pairs length (verified via molecular-weight size marker) were incised from the agarose gels for purification.

PCR Purification and Sanger Sequencing of PCR Amplicons

The agarose gel sections containing the amplified PCR products were purified using the NucleoSpin Gel and PCR Clean-up kit (Macherey-Nagel GmbH & Co., Duren, Germany). DNA was sequenced using a DNA sequencer (model 377; Applied Biosystems, Foster City, CA) as previously described (Eton Bioscience, Research Triangle Park, NC). The DNA templates used for the sequencing were at the concentration of 10-30ng/µL.

Analysis of Sanger Sequencing

Reference sequences were obtained from GenBank (NCBI reference sequence NM_015922.2) for the human *NSDHL* cDNA sequence and the mutant *NSDHL* cDNA sequence, which contained the mutations of interest**.** Consensus alignments and analysis of the sequencing results were completed using Molecular Biology 2.0 software (Benchling, San Francisco, CA). Separate consensus alignments were used for the Exon 4 and Exon 6 amplicons. Any mutations were analyzed to determine whether any amino acid change (or stop codon) resulted from the base pair change. Chromatograms were visualized using the FinchTV (version 1.5.0) software. Consensus multiple sequence alignment figures were created from relevant chromatograms using the Multalin software (http://multalin.toulouse.inra.fr/multalin/).

RESULTS

Successful PCR amplification of the three primer sets was confirmed with PCR reactions using HEK293T genomic DNA as a template (Figure 6). Due to difficulties in optimization of the extracted DNA, 16 samples from the original 20 tissue samples were selected as test samples for this study (labeled T1-T16). DNA was successfully extracted from all of the original five control samples (C1-C5). Confirmation that the plasmid contained the designed mutations was completed with sequencing of PCR amplicons (Figures 7, 8, 9). The plasmid was successfully spiked into a selected control (C5) tissue sample with exon 4 sense and antisense primers (Figure 8) but was unsuccessful with the exon 6 sense and antisense primer sets.

The mean age of the subjects from whom the oral VX samples were taken was 61.5 years old with a range of 15-92 years old (Table 1). The mean age of the control subjects was 25 years old with a range of 10-39 years old (Table 2). In the test group, 68.8% of the lesions were found in females (11 out of 16). In the control group, 3 of the 5 lesions were from female subjects (60.0%). The most common clinical impressions submitted with biopsies for the oral VX lesions were dysplasia, papilloma, and squamous cell carcinoma. The clinical impressions of the control samples were overwhelming "mucocele." This was confirmed by the UNC Oral Pathology Laboratory and Biopsy Service. 12 of the 16 test samples were listed as coming from the right side of patients (although the side of one of the remaining samples was not specified and two were from the patients' midline, encompassing both left and right sides). Health history information was not available for any of the subjects and it is unknown whether any of the subjects had a personal or family history of CHILD Syndrome.

Eight of the oral VX lesions (50%) (T1, T2, T4, T8, T9, T14-T16) exhibited a mutation in Exon 4 of the NSDHL gene that has been reported for CHILD Syndrome and was one of the mutations of interest for this study (Figure 10). Two of these eight lesions had a homozygous missense mutation at c.314 (C>T) at codon 105 (GCG > GTG) that results in the replacement of the amino acid alanine by valine at the codon (A105V) in the final protein product. The remaining six lesions had heterozygous missense mutations that included the same nucleotide substitution as the homozygous mutations (GCG>GTG) (Figures 8, 11). Neither the A105V mutation nor any other mutation was found in any of the remaining 8 oral VX lesions or in any of the 5 control samples (Figure 10).

Two of the oral VX lesions (12.5%) exhibited two mutations in Exon 6 of the NSDHL gene (Figure 12). One of the mutations has previously been reported for CHILD Syndrome and the other was a mutation that was previously reported in the literature associated with oral VX (Mehra et al., 2005). Both of these mutations were mutations of interest for this study. Both T4 and T16 had a heterozygous missense mutation at c.613 (G>A) at codon 205 (GGC>AGC) that results in the replacement of the amino acid alanine by serine at the codon (A205S) in the final protein product (Figure 13). This mutation was one of our mutations of interest and is associated with CHILD Syndrome. Additionally, each of the two lesions had a heterozygous missense mutation at c.596 (G>A) at codon 199 (CGC>CAC) that results in the replacement of the amino acid arginine by histidine at the codon (R199H) in the final protein product (Figure 13). This mutation was previously reported in two oral VX lesions but is not known to be associated with CHILD Syndrome (Mehra et al., 2005). These same two oral VX lesions also had the mutations mentioned previously in Exon 4 (see above). Neither the A205V or R199H mutations, nor any other

mutation was found in any of the remaining 14 oral VX lesions or in any of the 5 control samples (Figure 12). Additionally, neither of the other mutations of interest (A182P or Q201X) was found in these tissue samples or any of the test or control samples (Figure 12). A summary of the NSDHL mutational analyses is found in Table 3 and Table 4.

DISCUSSION

VX lesions are usually found in the oral mucosa, although extraoral locations, including, most commonly, the anogenital areas have been reported. The lesion, regardless of the location, has a distinct histopathological pattern of epithelial hyperplasia with aggregates of lipid-laden macrophages (often referred to as "foam cells") in the submucosa or papillary dermis. While other lesions, including oral mucoceles, contain foamy macrophages, VX is unique in that the cells are primarily found in the connective tissue. Evidence suggests that the characteristic lesions found in CHILD Syndrome, with their similar clinical and histological presentation, are strongly related to VX (Xu et al., 2015).

While the etiology of VX and foamy macrophage accumulation in the connective tissue remains unresolved, two prevailing theories have been proposed. Zegarelli et al suggested that epithelial degradation caused by a local irritant initiates formation of the characteristic foam cells. The epithelium becomes entrapped with the crypts within the stratified squamous epithelium and is not lost from the body. The entrapped epithelium then degenerates, eventually forming lipids. The products of this breakdown elicit an inflammatory response, explaining the neutrophil infiltrate that is often seen within the epithelium and a mostly chronic cell infiltrate in the submucosa (Zegarelli et al., 1975). It is unclear, however, how the initial crypts that would necessitate the entrapment of epithelial

cells might form. Additionally, Travis observed foam cell deposition in a multifocal VX in the upper aerodigestive tract of a child, in an area of little epithelial degradation. Noting that macrophages are known to produce a variety of growth factors (Nathan, 1987), it was suggested that the foam cells might play a role in inducing epithelial hyperplasia. Therefore, the accumulation of foam cells is the primary abnormality in the early lesion, and that increasing epithelial hyperplasia and inflammation are secondary (Travis et al., 1989).

Cholesterol is a major precursor of steroid hormones influencing embryonic and postnatal development and is vital to cell membranes. One of the later steps of its biosynthesis involves a 3b-hydroxysteroid dehydrogenase discovered only within the last 15 years and encoded by the NSHDL gene. The protein is found within the membranes of endoplasmic reticulum and on the surface of intracellular lipid storage droplets (Ohashi et al., 2003). It has been reported that instead of just being a vessel for lipid storage, the droplets themselves may be involved in the regulation of cholesterol biosynthesis. Normally, if an adequate amount of lipid droplets is produced for the local environment, NSHDL migrates from the endoplasmic reticulum to the lipid droplets and initiates a negative feedback to stop producing lipid droplets. However, with the introduction of a missense mutation associated with CHILD Syndrome (G205S, a mutation detected in our study) into the *NSDHL* gene, the protein was no longer functional and the negative feedback was lost, resulting in an increasing level of lipid droplets (Ohashi et al., 2003). This could account for the foam cells that are hallmark for VX lesions.

Additionally, abnormalities in cholesterol synthesis could prevent the establishment and upkeep of a complete cutaneous or epithelial barrier. It is believed that a non-functional NSDHL may cause the characteristic VX lesions of CHILD syndrome either through the

resulting lack of cholesterol, other sterols downstream of the block in biosynthesis, or by accumulations of intermediate products upstream of the resultant of NSDHL expression (Bornholdt et al., 2005).

Our study was inspired by a previous analysis by Mehra et al. in 2005 that concerned the *NSDHL* gene in cutaneous VX lesions. The characteristic lesions in cutaneous VX and CHILD syndrome have a similar appearance clinically. When evaluated histologically, they both feature foamy macrophages within dermal papilla. CHILD Syndrome is caused by a dysfunction of the NSDHL, caused by a mutation in the *NSDHL* gene. Therefore, Mehra et al. group was looking for mutations in cutaneous VX lesions that had previously been associated with CHILD Syndrome. To date, there have been over 20 mutations documented in the *NSHDL* gene (Mi et al., 2015). When their study was conducted over a decade ago, they focused on exons 4 and 6, as most of the documented cases involved mutations at these locations. Specifically, they were looking for mutations at codons 105, 182, and 205, which resulted in the amino acid changes A105V, A182P, and G205S associated with CHILD Syndrome. They also analyzed for an amino acid change at codon 210, which results in the amino acid change Q210X (a stop codon). While they were unable to find any mutations matching those reported for CHILD Syndrome, they did discover a novel missense mutation at codon 199 (R199H). We chose to do a similar study, but now looking for CHILD Syndrome mutations in *oral* VX lesions. Additionally, we wanted to screen for the presence of the somatic mutation that Mehra et al discovered (Mehra et al., 2005).

Early in the study, we encountered difficulty with successful extraction of the DNA from the archived tissue samples. The tissue samples, derived from oral biopsies, were often very small with a high paraffin to tissue ratio, which negatively affected DNA yields. We

eventually had to exclude four tissue samples from the study as the concentration and purity of the extracted DNA was poor and amplification with our primer sets was unsuccessful. We also were unsuccessful in generating sequencing results with the amplicon from our exon 6 primers when spiking the constructed plasmid into a control sample. This was meant to illustrate both the wild type and the mutation simultaneously and serve as positive control. This was, however, successful with the exon 4 primer set and it did mirror the heterozygous mutation that we discovered with 6 of the test samples.

In our test samples, eight samples (50%) displayed either a homozygous or heterozygous mutation at codon 105 (GCG>GTG), resulting in a replacement of alanine with valine in the final protein product (A105V). Two samples displayed a heterozygous mutation at codon 205 (GGC>AGC), resulting in a replacement of alanine by serine in the final protein product (G205S). These two different missense mutations are found in patients diagnosed with CHILD Syndrome. These same two test samples also displayed a heterozygous mutation at codon 199 (CGC>CAC), resulting in a replacement of arginine by histidine in the final protein product (R199H). This is the same novel somatic missense mutation encountered in the Mehra et al. study. It is notable that these two test samples are also included in the eight test samples that had a mutation at codon 105. The other mutations of interest for our study in exon 6 that had been previously reported with CHILD Syndrome (A182P, Q210X) were not found.

A previous investigation compared the NSDHL gene from humans to similar functional genes from other species (Bornholdt et al., 2005). When compared to other functionally similar genes, point mutations present on NSDHL at codon positions 105, 182, 205, and 210 correspond to areas that are highly conserved and required for protein function

(Figure 14). It is predicted that these genetic mutations influence NAD(P) binding within the active site of NSDHL. While disrupting substrate binding does not necessarily eliminate catalytic activity, it will significantly reduce the catalytic efficiency of the enzyme. Without a properly functioning enzyme, metabolism could be disrupted in a cell. Therefore, it is predicted that these newly discovered mutations in the NSDHL gene contribute to a reduction in in enzymatic activity of the NSDHL protein, possibly explaining their role in a pathologic state.

Most of the mutations found in this study were heterozygous, while two homozygous mutations were found in exon 4 of test samples 1 and 2. A comparison with known mutations in CHILD Syndrome shows similar variability (König et al., 2000, Hummel et al., 2003, Bittar et al., 2006). Patients diagnosed with CHILD Syndrome can display a wide range of phenotypes ranging from very mild skin lesions to the classic manifestations of the syndrome.

In humans, female cells carry two X-chromosomes and males carry an X and Y chromosome. In the female, one of the X chromosomes is silenced at random with regard to parental origin, a process termed X-inactivation, or lyonization. This randomization occurs early in embryonic development and is maintained through all cell divisions. X-inactivation results in every female consisting of a mosaic of two different cell populations (where either the paternal or maternal derived X-chromosome is inactivated). (Deng et al., 2014). In X-linked diseases caused by mutation, as is the case with CHILD Syndrome, males are usually affected to a significantly greater degree, as they have only one X-chromosome. In males, CHILD Syndrome is overwhelmingly male lethal. In our study, the only homozygous mutations (C>T at codon 105) were found in males. A more variable phenotype is usually

seen in females. In CHILD Syndrome, heterozygous carriers for the disease can display mild symptoms (Yu et al., 2018). This variability and the common clinical presentation primarily on one side of the body (there seems to be a prevalence for the right side (Hummel et al., 2003) has been explained by mosaicism by lyonization (Hashimoto et al., 1998).

However, even if an X-linked mutation results in the dysfunction or absence of a protein, possibly affecting the growth or potentially causing the death of a particular cell, the surrounding environment may provide compensating proteins or signals which may allow masking, and function may be restored. Usually X-inactivation is random, but X-chromosome inactivation skewing can occur, where the inactivation of one X chromosome is favored over the other. Mouse models have skewing of X inactivation in the *NSDHL* gene as adults (McLarren et al., 2010). Skewing can be caused by chance or directed by genes. In addition, the selective pressure for skewing does not appear to be the same in all tissues or at all developmental stages and skewing can be affected by aging. Many studies have found that skewing is more prevalent in elderly women (Deng et al., 2014).

While CHILD Syndrome has usually presented as a sporadic manifestation, there are eight documented cases of mother to daughter transmission. In one particular case, the proband presented with the spectrum of CHILD Syndrome symptoms, yet her mother and grandmother were only affected with a minor scaling lesion on one finger and toe, respectively. Molecular analyses confirmed *NSDHL* mutations. The authors concluded that the wide range of manifestations might be the result of either extreme lyonization or genetically induced skewing of X chromosome inactivation. Furthermore, they deemed it possible that many cases of CHILD Syndrome have not been diagnosed and may have a

familial origin (Bittar et al, 2006). No familial aggregation of Verruciform xanthoma has been reported.

The subjects with our mutations had ages ranging from 15-92 years old (mean age 61.5 years). Discounting Test Sample 16 from a 15-year old male patient, our range was 43-92 years old, with a mean age of 64.6 years. Furthermore, it is interesting that all of the heterozygous mutations that we found in our test samples were derived from female patients, except one (the 15-year old male). Both of the homozygous mutations were found in 67- and 89-year old men. Comparing our test subjects to CHILD Syndrome patients, male patients are extremely rare (only one has been documented). In the reported male patient, he had an otherwise normal karyotype, but was heterozygous for "wild-type" and mutant alleles in cultured fibroblasts from affected cutaneous lesions. It has been proposed that the mutation represented an early post-zygotic event.

A final observation was that, as is found with CHILD Syndrome, most of our lesions with mutations were found specifically on the right side of the subject (5 out of 8, with two of the other 8 samples presenting at the midline, and one from the left side) (Table 1).

While it is tempting to make direct comparisons between diagnosed CHILD Syndrome patients and our oral VX patients, it is important to note that no germline testing was conducted for any of the patients from whom we derived tissue samples.

CONCLUSIONS

We were able to demonstrate that missense mutations found in the *NSHDL* gene known to be associated with CHILD Syndrome can be identified in oral VX lesions through DNA sequencing. Because we only selected specific exons for this study, to mirror a

previous study that addressed cutaneous VX lesions, it is possible that additional exons of the *NSDHL* gene may harbor additional identified CHILD Syndrome-associated mutations. Additional studies should include sequencing of additional exons of the *NSDHL* gene. In addition, germline testing of affected patients may be beneficial. That we were able to identify these mutations (and a previously reported somatic mutation unrelated to CHILD Syndrome) may contribute to an etiologic theory based on genetics for VX. Further studies may contribute to further efforts to evaluate for risk for NSHDL mutation associated diseases, including CHILD Syndrome or CK Syndrome in families of subjects with oral VX.

Table 1. Clinicopathologic Characteristics of Test Samples.

SAMPLE	AGE/SEX	ANATOMICAL LOCATION	CLINICAL IMPRESSION(S)
T1	67/M	Right retromolar pad	Verrucous hyperplasia, papilloma, squamous cell carcinoma
T2	89/M	Right mandibular buccal attached gingiva (Tooth #30)	Leukoplakia
T3	63/F	Right posterior mandibular buccal vestibule	Verrucous hyperplasia, papilloma, squamous cell carcinoma
T4	92/F	Right palatal (Tooth #3)	Fibroma
T5	42/F	Right palatal (Tooth #3)	Not provided
T6	70/M	Right buccal mucosa (Arch unspecified)	Not provided
T7	59/F	Right palatal (Tooth #3)	Papilloma
T8	76/F	Palate (Side unspecified)	Irritation fibroma
T9	81/F	Left buccal mucosa (Tooth #19)	Epithelial dysplasia
T10	62/M	Midline mandibular lingual (Teeth #24,25)	Verruciform xanthoma
T11	69/F	Right buccal mucosa	Dysplasia, squamous cell carcinoma
T12	56/F	Right lateral of tongue	Papilloma
T13	43/F	Right (buccal or palatal not specified) (Tooth #2)	Hyperkeratosis, dysplasia
T14	45/F	Right mandibular buccal mucosa (Tooth #31)	HPV lesion
T15	55/F	Teeth #24,25 (Buccal/lingual gingiva unspecified)	“Wart”
T16	15/M	Right maxillary buccal papilla (Teeth #6/7)	Not provided

Table 2. Clinicopathologic Characteristics of Control Samples.

SAMPLE	AGE/SEX	ANATOMICAL LOCATION	CLINICAL IMPRESSION(S)
C1	28/M	Right lower lip	Mucocele
C2	39/M	Right lower lip	Mucocele, fibroma
C3	17/F	Lower lip (Side unspecified)	Mucocele, fibroma
C4	31/F	Right lower lip	Mucocele
C5	10/F	Lower lip (Side unspecified)	Mucocele, fibroma

Table 3. Summary of NSDHL Mutational Analysis in Oral VX Test Samples.

SAMPLE	MUTATIONS		NUCLEOTIDE AFFECTED	TYPE OF MUTATION(S)	RESULTANT AA CHANGE	ASSOCIATED MUTATION	
	EXON 4	EXON 6				CHILD SYNDROME	ORAL VX
T1	YES	No	c.314	C > T	Alanine > Valine	YES	No
T2	YES	No	c.314	C > T	Alanine > Valine	YES	No
T3	No	No	--	--	--	--	--
T4	YES	YES	c.314 c.596 c.613	C > T G > A G > A	Alanine > Valine Arginine > Histidine Glycine > Serine	YES No YES	No YES No
T5	No	No	--	--	--	--	--
T6	No	No	--	--	--	--	--
T7	No	No	--	--	--	--	--
T8	YES	No	c.314	C > T	Alanine > Valine	YES	No
T9	YES	No	c.314	C > T	Alanine > Valine	YES	No
T10	No	No	--	--	--	--	--
T11	No	No	--	--	--	--	--
T12	No	No	--	--	--	--	--
T13	No	No	--	--	--	--	--
T14	YES	No	c.314	C > T	Alanine > Valine	YES	No
T15	YES	No	c.314	C > T	Alanine > Valine	YES	No
T16	YES	YES	c.314 c.596 c.613	C > T G > A G > A	Alanine > Valine Arginine > Histidine Glycine > Serine	YES No YES	No YES No

Table 4. Summary of NSDHL Mutational Analysis in Control Samples.

SAMPLE	MUTATIONS		NUCLEOTIDE AFFECTED	TYPE OF MUTATION(S)	RESULTANT AA CHANGE	ASSOCIATED MUTATION	
	EXON 4	EXON 6				CHILD SYNDROME	ORAL VX
C1	No	No	--	--	--	--	--
C2	No	No	--	--	--	--	--
C3	No	No	--	--	--	--	--
C4	No	No	--	--	--	--	--
C5	No	No	--	--	--	--	--

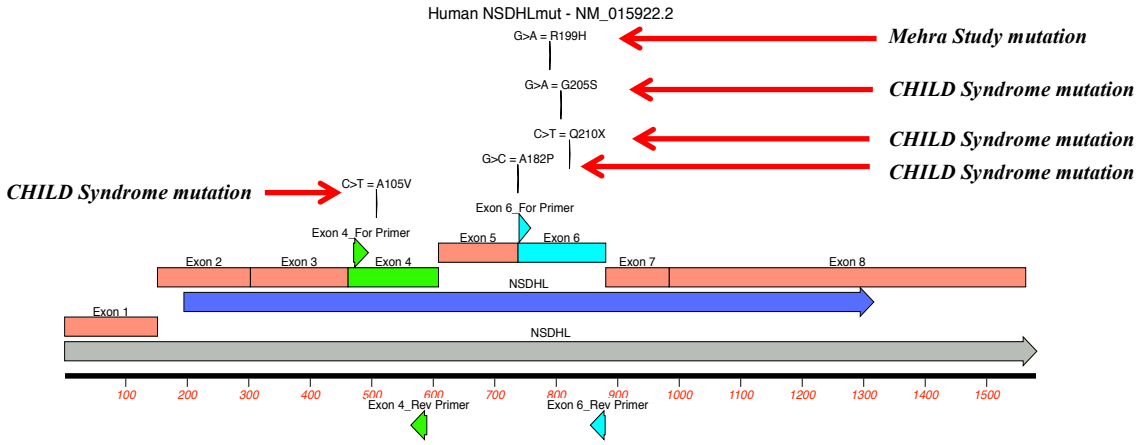

Figure 4. NSDHL Mutations of Interest. Four known germline mutations associated with CHILD Syndrome in Exon 4 and Exon 6 of the NSDHL gene and one somatic mutation not known to be associated with CHILD Syndrome in Exon 6 discovered in the 2005 Mehra Study. Primer design noted.

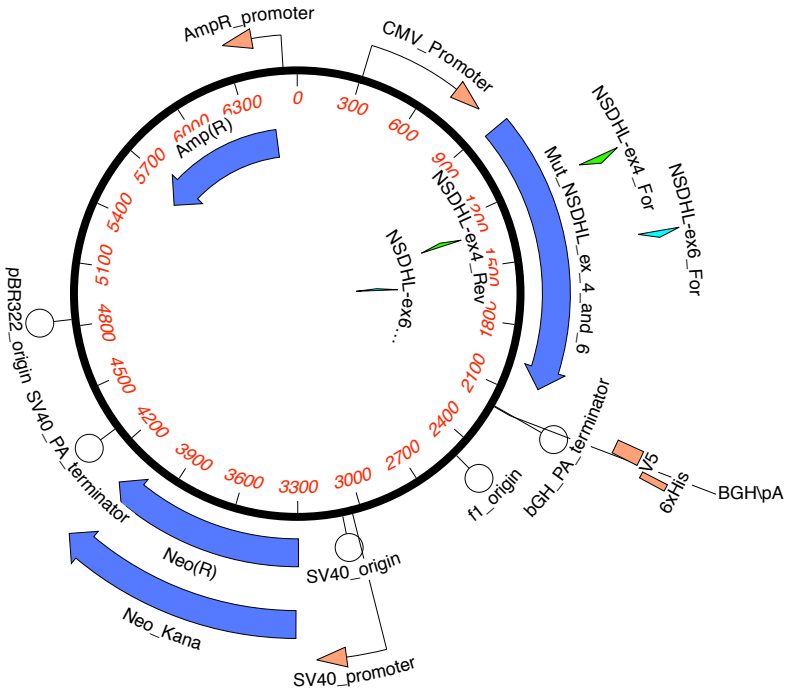

Figure 5. Plasmid Engineered with Human HSDHL Mutant Template. Invitrogen GeneArt Synthesis, Germany.

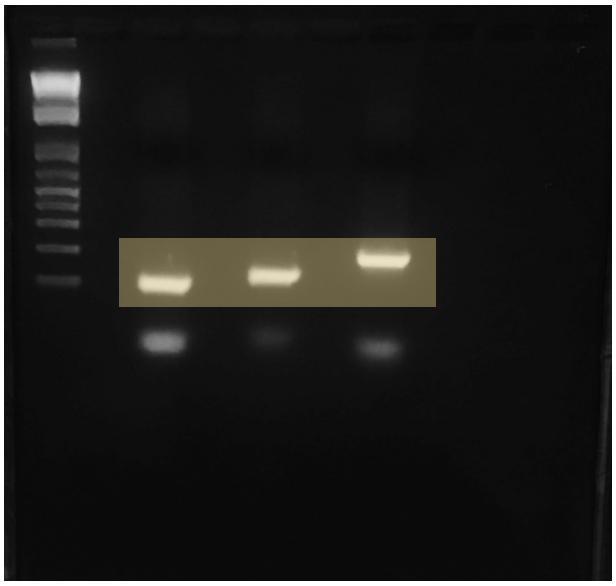

Figure 6. Study Primer Pairs with HEK293T DNA to Confirm PCR Amplification. Expected size: 119bp NSDHL Exon 4 F/R; 140bp NSDHL Exon 6 F/R; 206bp NSDHL Intron 5F/Exon 6R.

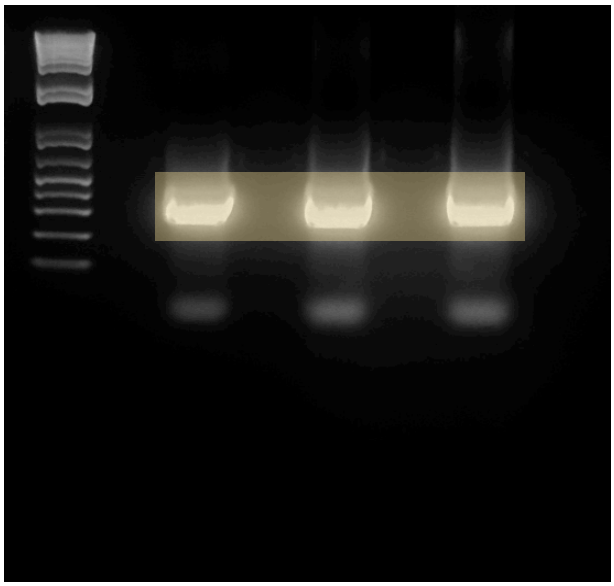

Figure 7. Student Exon 4 sense/Exon 6 antisense Primers with Constructed Plasmid. Expected size: 409bp.

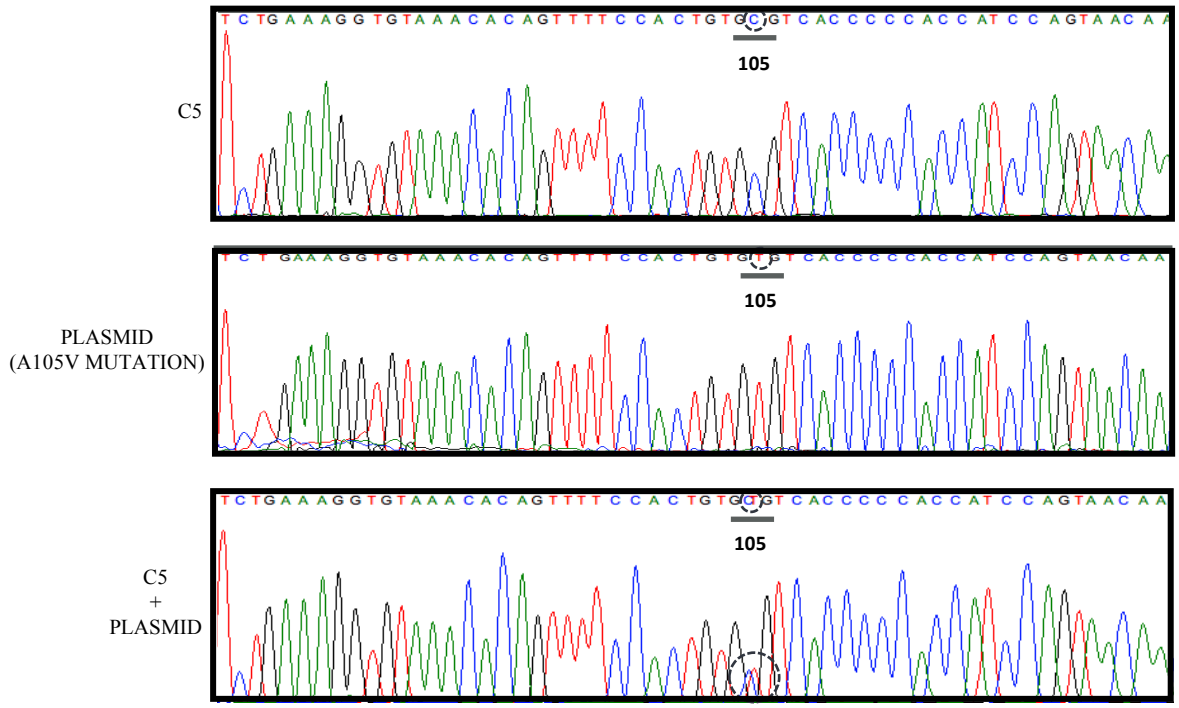

Figure 8. Sanger Sequencing, Exon 4 Amplicons. Controls.

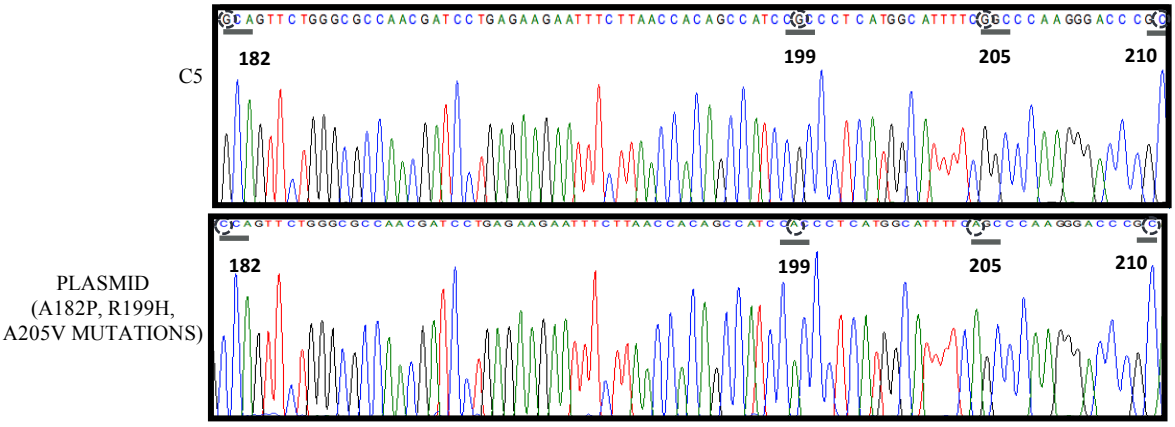

Figure 9. Sanger Sequencing, Exon 6 Amplicons. Controls.

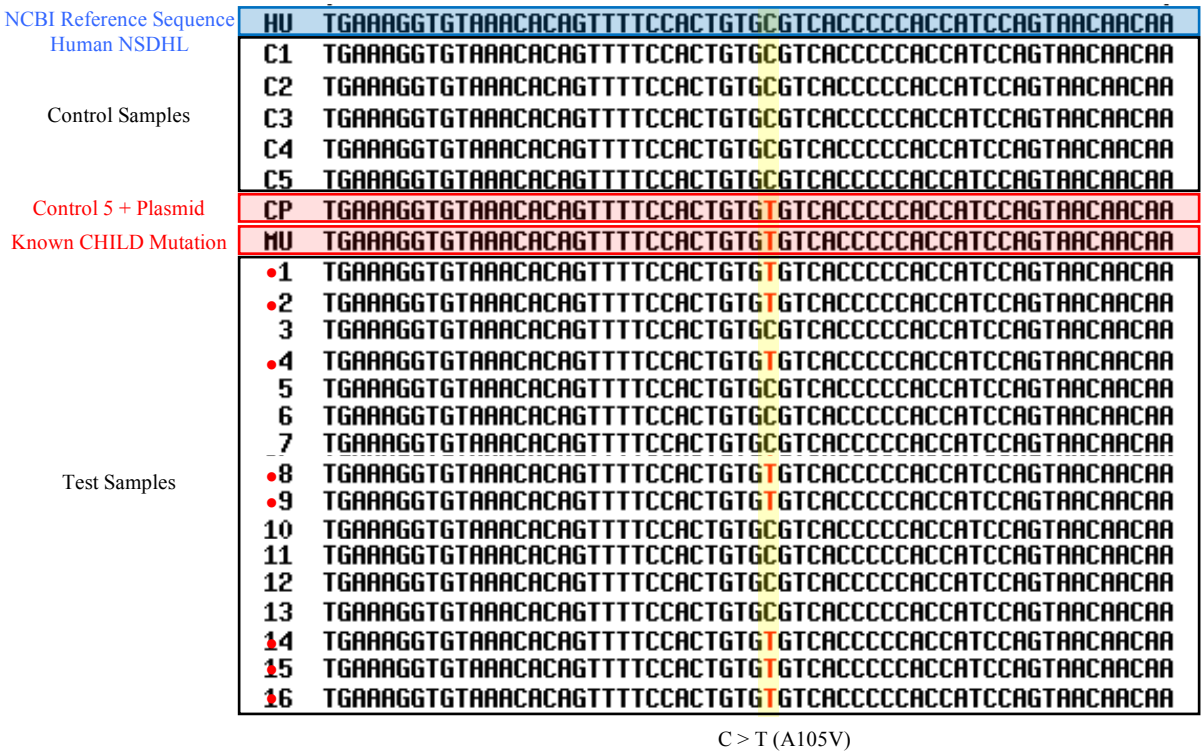

Figure 10. Consensus Multiple Sequence Alignment of Exon 4 Sanger Sequencing. Red circles indicate presence of mutation C > T (A105V) in test samples.

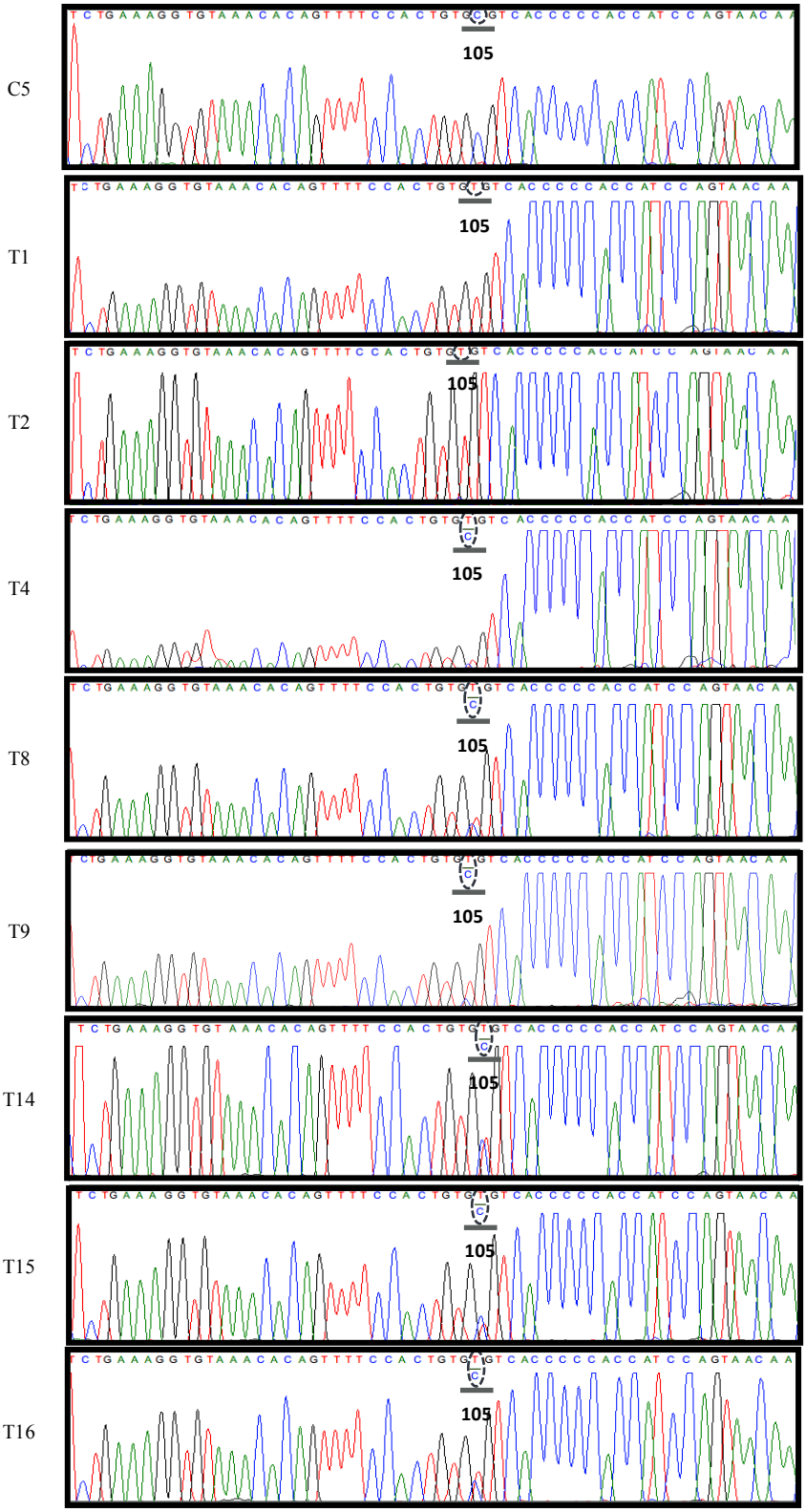

Figure 11. Sanger Sequencing, Exon 4 Amplicons. Test Sample Mutations.

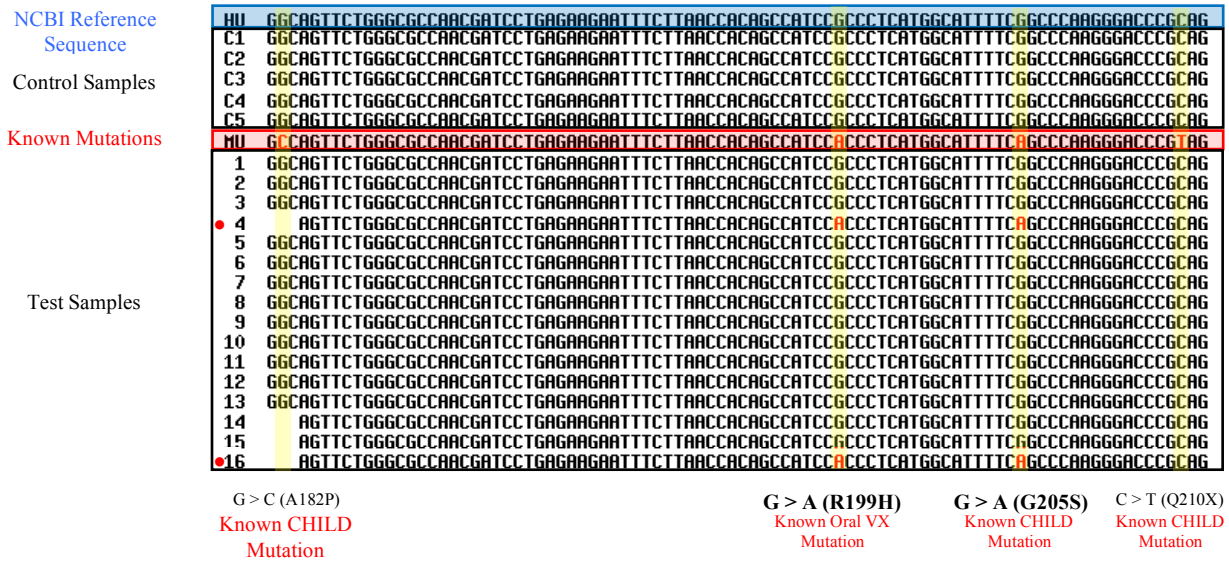

Figure 12. Consensus Multiple Sequence Alignment of Exon 6 Sanger Sequencing. Red circles indicate presence of mutation G > A (R199H) and G > A (G205S) in test samples.

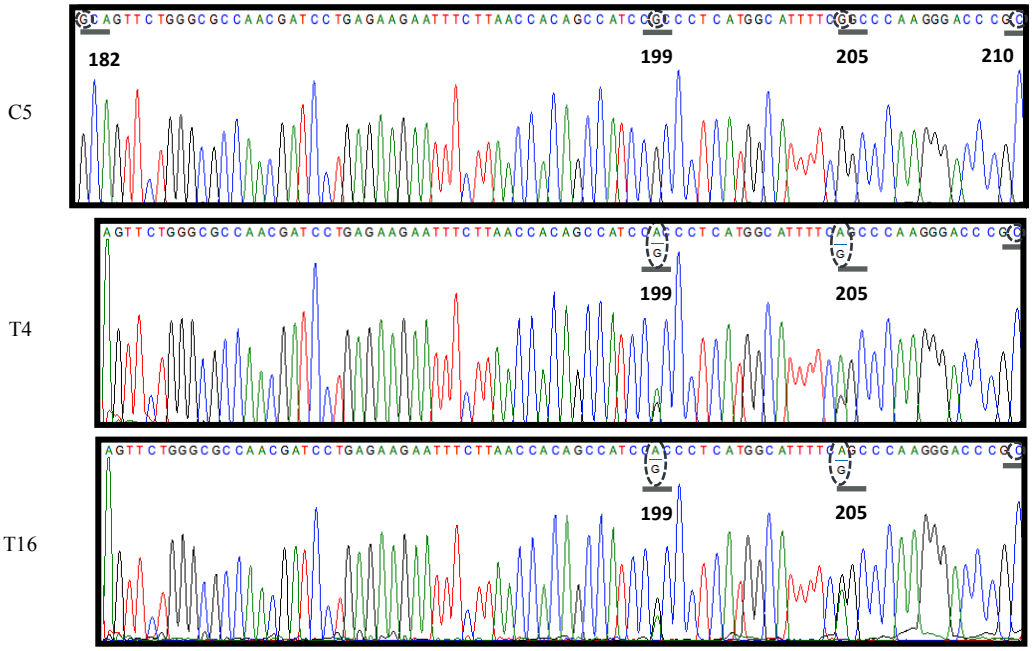

Figure 13. Sanger Sequencing, Exon 6 Amplicons. Test Sample Mutations.

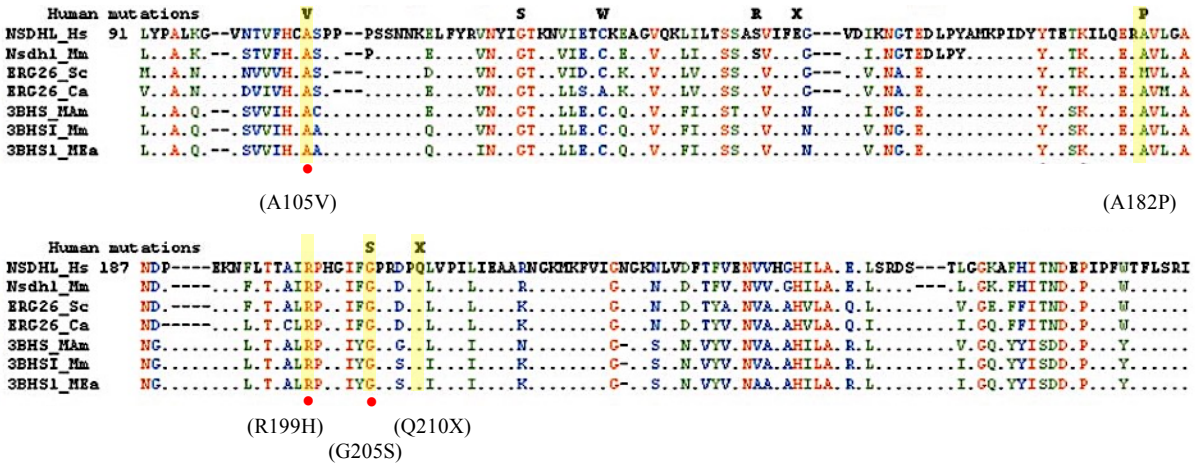

Figure 14. Multiple Sequence Alignments Displaying Mutations of Interest in Human NSDHL Preferentially Exchange Conserved Amino Acids Across Species. From the top, in order: human, mouse, Saccharomyces cerevisiae, Candida albicans, Macaca mulatta, mouse, Mesocricetus auratus. Identical amino acids are shown in red, mutations observed in black, strongly similar amino acids in green, weak similarity is blue. Black dots represent non-conserved positions (Bornholdt et al., 2005). Also illustrated is the R199H mutation from the 2005 Mehra study. Red circles have been added to denote the mutations found in our test samples.

REFERENCES

Bittar M, Happle R, Grzeschik K-HH, Leveleki L, Hertl M, Bornholdt D, et al. CHILD syndrome in 3 generations: the importance of mild or minimal skin lesions. Arch Dermatol. 2006;142(3):348-351

Bornholdt, König, Happle, Leveleki, Bittar, Danarti, et al. Mutational spectrum of NSDHL in CHILD syndrome. Journal of Medical Genetics. 2005;42(2):e17.

Deng X, Berletch JB, Nguyen DK, Disteche CM. X chromosome regulation: Diverse patterns in development, tissues and disease. Nature Reviews.Genetics. 2014;15(6):367-378.

Hashimoto K, Prada S, Lopez AP, Hoyos JG, Escobar M. CHILD syndrome with linear eruptions, hypopigmented bands, and verruciform xanthoma. Pediatr Dermatol. 1998;15(5):360-366.

Hummel M, Cunningham D, Mullett C, Kelley R, Herman G. Left-sided CHILD syndrome caused by a nonsense mutation in the NSDHL gene. Am J Med Genet A. 2003;122A(3):246-251.

König A, Happle R, Bornholdt D, Engel H, Grzeschik KH. Mutations in the NSDHL gene, encoding a 3beta-hydroxysteroid dehydrogenase, cause CHILD syndrome. Am J Med Genet. 2000;90(4):339-346.

Kurban M, Abbas O, Ghosn S, Kibbi A. Late evolution of giant verruciform xanthoma in the setting of CHILD syndrome. Int Congr Ser. 2010;27(5):551-553.

Mehra S, Li L, Fan C-YY, Smoller B, Morgan M, Somach S. A novel somatic mutation of the 3beta-hydroxysteroid dehydrogenase gene in sporadic cutaneous verruciform xanthoma. Arch Dermatol. 2005;141(10):1263-1267

Mi X, Luo M, Guo L, Zhang T, Qiu X. CHILD syndrome: case report of a Chinese patient and literature review of the NAD[P]H steroid dehydrogenase-like protein gene mutation. Int Congr Ser. 2015;32(6):e277–e282.

Nathan C. Secretory products of macrophages. J Clin Invest. 1987;79(2):319-326.

Ohashi M, Mizushima N, Kabeya Y, Yoshimori T. Localization of mammalian NAD(P)H steroid dehydrogenase-like protein on lipid droplets. J Biol Chem. 2003;278(38):36819-36829.

Travis WD, Davis GE, Tsokos M, Lebovics R, Merrick HF, Miller SP, et al. Multifocal verruciform xanthoma of the upper aerodigestive tract in a child with a systemic lipid storage disease. Am J Surg Pathol. 1989;13(4):309-316.

Xu X, Huang L, Wang Q, Sun J. Multiple verruciform xanthomas in the setting of congenital hemidysplasia with ichthyosiform erythroderma and limb defects syndrome. Pediatr Dermatol. 2015;32(1):135-137.

Yu X, Zhang J, Gu Y, Deng D, Wu Z, Bao L, et al. CHILD syndrome mimicking verrucous nevus in a Chinese patient responded well to the topical therapy of compound of simvastatin and cholesterol. J Eur Acad Dermatol. 2018; Jan 17. doi: 10.1111/jdv.14788.

Zegarelli DJ, Zegarelli-Schmidt EC, Zegarelli EV. Verruciform xanthoma. Further light and electron microscopic studies, with the addition of a third case. Oral Surg Oral Med Oral Pathol. 1975;40(2):246-56.